Battery charger with a capacitor-diode clamped LLC resonant converter

[†]C. –W. Tsang*, [†]C. Bingham, [††]M.P. Foster, [††]D.A. Stone, [†††]J.M.Leach

[†]*University of Lincoln, Lincoln School of Engineering, Brayford Pool, Lincoln, UK*
[††]Electronic and Electrical Engineering, The University of Sheffield, Sheffield, UK
[†††]*Castlet Ltd, 14 Crofton Drive,Allenby Road Inductrial Estate, LN3 4NR, UK*
Email: ctsang@lincoln.ac.uk

Keywords: LLC resonant converter, capacitor-diode clamp, battery charger, multi-stage converter.

Abstract

The paper proposes a novel battery charger through use of two serially-connected LLC resonant converters. The first stage utilises a capacitor-diode clamped LLC resonant converter which allows operation in both constant voltage (CV) and constant current (CC) modes, as found in most battery chargers, to be realised, whilst the second stage provides the necessary gain and line and load regulation. A design example is included that demonstrates the resulting converter topology operating under the full battery charging conditions and its inherent current-limiting capability. Experimental results are used to validate the underlying approach.

1 Introduction

Research on battery charging power converters has increased dramatically due to the requirement for electric vehicles (EVs) and other alternative electric-based energy harvesting/integration schemes that require battery energy storage. The many requirements for such converters include high efficiency operation with minimal size and mass, which has created significant challenges. Many alternative topologies have been proposed, including multi-phase boost converters and multi-level converters [1, 2]. However, a number of the most promising topologies are based on the LLC resonant converters [3], which have become popular due to their soft-switching characteristics that facilitate reduced switching losses and hence improve the overall converter efficiency. However, one of the main impediments to their widespread adoption is that at their nominal operating point (the independent load point) an excessive current can flow if the load is not controlled, potentially leading to damage of both the converter and the load.

Overcurrent protection for this converter can be achieved by reducing the MOSFET conduction times or increasing the operating frequency, requiring current sensors to detect the overload condition and controller to perform the corrective actions [4]. An alternative solution, using a capacitor-diode clamp [5], changes the resonant converter characteristics by switching in or out the resonant tank components. This scheme performs the current limiting as soon as the overload current occurs without the need or added latency of a feedback mechanism.

The voltage gain characteristic of the capacitor-diode clamped LLC resonant converter is shown in Fig. 1. The gain is unaffected for any load condition below the designated maximum. As soon as the overload condition is reached, the gain is attenuated according. This unique characteristic is utilised in this paper to obtain the desired V-I characteristics required for battery charging.

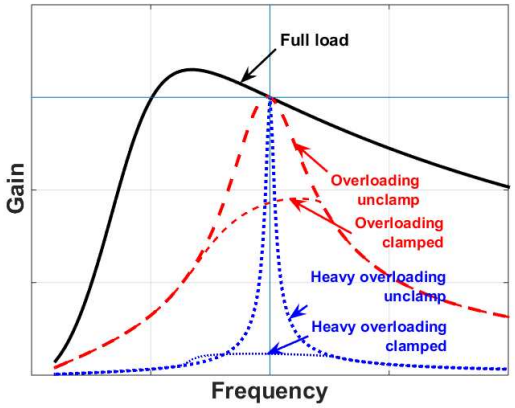

Fig. 1: Capacitor-diode clamped LLC resonant converter gain characteristics.

Dependent on the type of battery being charged, a number of charging regimes are required to be fulfilled by the battery charger. For lead-acid battery, these are the constant current (CC), constant voltage (CV) and float charge (FC) modes. The first two are the minimum required for this type of battery, with the charging profile is shown in Fig. 2.

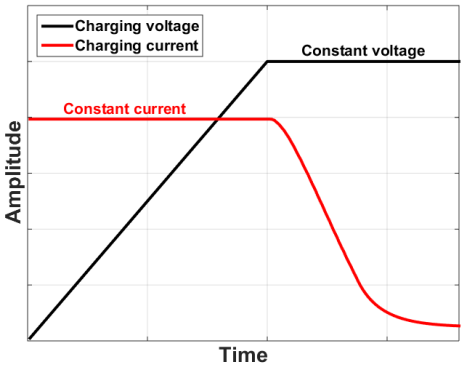

Fig. 2: Lead-acid battery charging profile.

The battery is initially charged using a constant current mode, when most of charge is replenished. The terminal voltage rises as the battery is being charged and the charging mode is switched to the constant voltage mode when the terminal voltage reaches the set voltage, typically 2.3 V – 2.45 V per cell. The selection of switching voltage is a compromise between battery life and capacity (see [7]). The CV mode ends when the charging current drops to a pre-determined level.

Here, the paper proposes a multi-stage battery charger where the first stage is a capacitor-diode clamped LLC resonant converter and the second stage is a traditional LLC resonant converter. The first stage operates in constant voltage mode when the battery voltage is at or above the pre-set level (V_{bat}), and in constant current mode when it is below V_{bat}. The second stage LLC resonant converter transformer turns ratio is adjustable to allow switching between the two charging modes, and for line and load regulation. Consequently, the converter does not require traditional dual voltage- and current-regulation controllers [6] and is always operating at or closed to the Load Independent Point (LIP), achieving both high robustness and efficiency.

2 Multi-stage LLC resonant converters

The first and second stages of the proposed multi-stage LLC resonant converters are shown in Fig. 3 (a) and (b) respectively.

The first stage is a capacitor-diode clamped LLC resonant converter and contains the three main functional parts found in a traditional LLC resonant converter: (i) a DC chopper formed by two complementary switched (MOSFETs) S_1 and S_2, converting the DC input voltage, V_i, into a pulsated waveform, (ii) a resonant tank formed by inductors and capacitors L_p, L_s and C_c, which allows the fundamental component of the square waveform to pass through, (iii) transformer, bridge rectifier and output filter formed by diodes $D_1 - D_4$ and capacitor C, converting the transformer secondary AC waveform into the DC output. Also included are the two diodes D_{c1} and D_{c2} which act to clamp the voltage across the resonant capacitor, V_C, to the input voltage rail for current-limiting purposes.

The second stage is a traditional LLC resonant converter with an additional path on the primary side of the transformer to enable the transformer turns ratio to be adjusted. The two paths are controlled by switches S_{p1} and S_{p2}. Since both the leakage and magnetising inductances and equivalent load condition are functions of the transformer winding turns and turns ratio, an additional resonant capacitor in included in the path to keep the resonant frequency fixed.

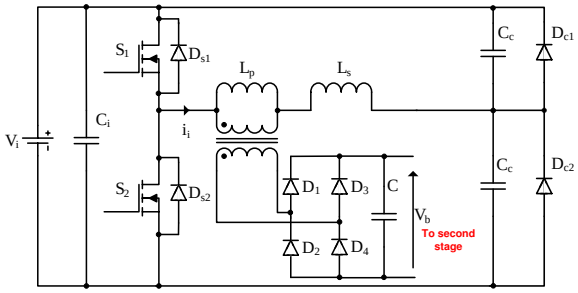

(a)

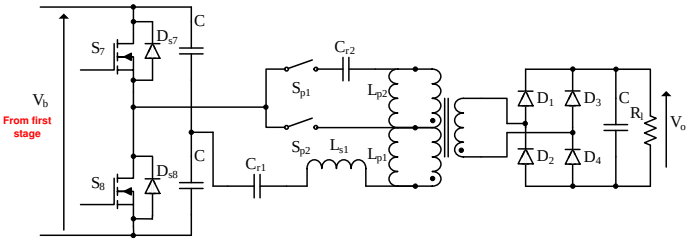

(b)

Fig. 3: Schematic of the proposed multi-stage LLC resonant converter. (a) First stage (b) Second stage

2.1 Equivalent circuit model

LLC resonant converter is most commonly modelled using first harmonic approximation (FHA) analysis, where the input current (I_i) and output voltage (V_o) are approximated, respectively, by (1) and (2) (note: ideal diode characteristics are assumed in the analysis).

$$I_i = \frac{2V_i}{\pi Z_1} \tag{1}$$

$$V_o = \frac{\pi I_i (R_{eq} || sL_p)}{4n} \tag{2}$$

where $Z_1 = R_{eq}||(sL_p) + sL_s + 1/(2sC_c)$ is the input impedance of the resonant circuit and $s = j\omega_s$ is the complex frequency. $R_{eq} = ((8n^2R_l)/\pi^2)$ is the equivalent resistance presented by the rectifier, output filter and load reflected through a transformer turn ratio n.

As an aid to studying the converter's general behaviour, irrespective of the resonant tank components selection, the nominalised gain M_g is commonly used. This is obtained by substituting (1) into (2), and rearranging in terms of $(2nV_o)/V_i$, then normalising against the three parameters viz. inductor ratio $A = L_p/L_s$, loaded quality factor $Q = \sqrt{L_s/C_r}/R_{eq}$ and normalised switching frequency (wrt. the series resonant frequency) $f_n = f_s/f_o$. The result is (3):

$$M_g = \frac{2nV_o}{V_i} = \frac{Af_n{}^2}{Af_n{}^2 + f_n{}^2 - 1 + j(f_n{}^3 QA - f_n QA)} \tag{3}$$

With the capacitor C_c excited by a sinusoidal input current, its voltage at any given instant is found using (4). Substituting $\omega_s t$ for θ (where $\omega_s = 2\pi f_s$ being the angular switching frequency and t is time), the capacitor voltage v_c at any θ is given by (5):

$$v_C(t) = \frac{1}{2C_c}\int I_i sin(\omega_s t)\, dt \; = -\frac{I_i}{2\omega_s C_c} cos(\omega_s t) + V_n \tag{4}$$

$$v_C(\theta) = -\frac{I_i}{2\omega_s C_c} cos(\theta) + V_n \tag{5}$$

where V_n is the initial condition for a given conduction state starting at $\theta = n$.

The DC blocking property of the capacitors, or the DC component of the DC chopper (half-bridge) is superimposed onto v_c as in (6):

$$v_C(\theta) = -\frac{I_i}{2\omega_s C_c} cos(\theta) + \frac{V_i}{2} \tag{6}$$

With the inclusion of the capacitor-diode clamp, the sinusoidal voltage across the capacitor is clipped whenever its voltage exceeds the range of the input voltage, as shown in the example given in Fig. 4. The equivalent diode-clamp/capacitor impedance Z_c is found through a describing function technique using the following three steps.

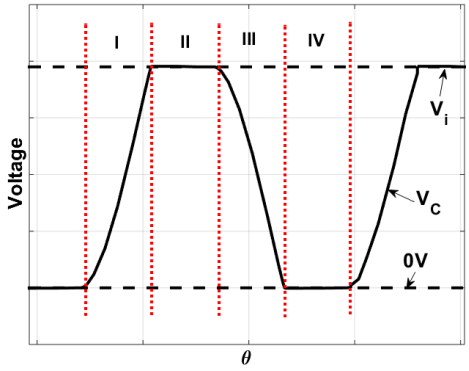

Fig. 4: Resonant capacitor voltage waveform.

Step 1: identify the piecewise equation describing the capacitor voltage v_c.

Within a single cycle, there are two intervals when the diode-clamp is inactive, hence there are two initial conditions V_n. In the first interval I $(0 < \theta \leq \delta)$, the capacitor voltage, v_c, is zero at the start. By substituting the known quantities in (5), the initial condition is found from (7):

$$V_0 = \frac{I_i}{2\omega_s C_c} \tag{7}$$

During the interval III $(\pi < \theta \leq \pi + \delta)$, the voltage across the resonant capacitor has been charged to V_i and begins discharging towards 0 V. Using the same procedure as above, the initial condition for this interval is found from (8),

$$V_\pi = V_i - \frac{I_i}{2\omega_s C_c} \tag{8}$$

Combining the two initial conditions in (7) and (8) with (5) and accounting for the two clamping levels, the piecewise description of the capacitor voltage is given by (9):

$$v_C(\theta) = \begin{cases} \frac{I_i}{2\omega_s C_c}(1 - cos(\theta)) & 0 < \theta \leq \delta \\ V_i & \delta < \theta \leq \pi \\ V_i - \frac{I_i}{2\omega_s C_c}(1 + cos(\theta)) & \pi < \theta \leq \pi + \delta \\ 0 & \pi + \delta < \theta \leq 2\pi \end{cases} \tag{9}$$

The diode-clamp non-conduction angle, δ, is found by evaluating the change in capacitor voltage over the diode-clamp non-conduction period. At the end of the first interval, the capacitor voltage has charged to V_i. Hence, substituting $v_C(\delta) = V_i$ into (9) and rearranging gives,

$$\delta = cos^{-1}\left(1 - \frac{2\omega_s C_c V_i}{I_i}\right) \tag{10}$$

Step 2: develop a describing function for v_c through extracting the fundamental component with Fourier analysis and the piecewise equation in (9).

The Fourier series representation of a repetitive waveform is given in (11) where $f(t)$ is the original time domain signal $v_c(t)$, a_0 is the DC component, a_n & b_n are harmonic components of the waveform and T is the period of one cycle:

$$\begin{aligned} f(t) &= a_0 + \textstyle\sum_{n-1}^{\infty}\left(a_n cos(n\omega_s t) + b_n sin(n\omega_s t)\right) \\ a_0 &= \frac{1}{2\pi}\int_{-T/2}^{T/2} f(t)dt \\ a_n &= \frac{1}{\pi}\int_{-T/2}^{T/2} f(t)cos(n\omega_s t)dt \\ b_n &= \frac{1}{\pi}\int_{-T/2}^{T/2} f(t)sin(n\omega_s t)dt \end{aligned} \tag{11}$$

For AC equivalent circuit analysis, the DC component, a_0 can be ignored, and since the converter's behaviour is dominated by the fundamental component, the Fourier series can be simplified to a describing function as follows:

$$\begin{aligned} f(\theta) &= a_1 cos(\theta) + b_1 sin(\theta) \\ a_1 &= \frac{1}{\pi}\int_0^{2\pi} f(\theta)cos(\theta)d\theta \\ b_1 &= \frac{1}{\pi}\int_0^{2\pi} f(\theta)sin(\theta)d\theta \end{aligned} \tag{12}$$

By substituting (9) into (12) the fundamental component of v_c is given by:

$$\begin{aligned} v_C(\theta) = &\left[\frac{2}{\pi}V_i\, cos(\delta) + \frac{I_i}{2\pi\omega_s C_c}\left(1 + cos(\delta)\,(cos(\delta) - 2)\right)\right] sin(\theta) \; + \\ &\left[-\frac{2}{\pi}V_i\, sin(\delta) - \frac{I_i}{2\pi\omega_s C_c}\left(\delta + sin(\delta)(cos(\delta) - 2)\right)\right] cos(\theta) \end{aligned} \tag{13}$$

Step 3: obtain the equivalent impedance for diode-capacitor combination by dividing (13) by the sinusoidal input current $i_i = I_i \sin(\theta)$.

The equivalent impedance of the diode-capacitor combination is obtained by applying the transform $cos(\theta) = jsin(\theta)$ and then dividing by resonant current, as follows:

$$Z_C = \left[\frac{2V_i}{\pi I_i} cos(\delta) + \frac{1}{2\pi\omega_s C_c}\left(1 + cos(\delta)\,(cos(\delta) - 2)\right)\right] + j\left[-\frac{2V_i}{\pi I_i} sin(\delta) - \frac{1}{2\pi\omega_s C_c}\left(\delta + sin(\delta)(cos(\delta) - 2)\right)\right] \quad (14)$$

Substituting Z_c into the FHA model then provides (15), where the effect of the diode-clamp is accommodated by allowing the magnitude of the resonant tank current under clamping (i.e. overload) to be obtained. The output voltage can be found by substituting (15) into (2).

$$I_i = \frac{2V_i}{\pi Z_2} \quad (15)$$

where $Z_2 = R_{eq}||sL_p + sL_s + Z_c$, and s and R_{eq} are as given previously.

Since (15) cannot be solved analytically owing to the dependence on I_i for determining both δ and Z_c, an iterative procedure similar to that employed in [3] is used: the value of resonant tank current is first estimated using (1) by assuming the diode-clamp is inactive. Once I_i is obtained, the non-conduction angle, δ, and capacitor-diode clamp equivalent impedance, Z_c, are found using (10) and (14), after which a refined value for I_i is found using (15). The refinement of δ, Z_c and I_i are achieved through an iterative loop until they converge. Similar to the inactive diode-clamp case (i.e. normal non-current limited operation), the converter gain with an active diode-clamp, $M_{g(clmp)}$, is obtained through substituting (15) into (1) and rearrange in terms of $(2nV_o)/V_i$, as in (16), and substituting $s = j\omega$, $Z_c = R + jX$ (where R and X are the real and imaginary part of Z_c in (17) respectively), and introducing the $j\omega C_r$ term into both the numerator and denominator, again as in (17):

$$M_{g(clmp)} = \frac{V_o}{V_i} 2n = \frac{R_{eq}||sL_p}{R_{eq}||sL_p + sL_s + Z_c} \quad (16)$$

$$M_{g(clmp)} = \frac{j^2\omega^2 L_p C_r}{j^2\omega^2 L_p C_r + \frac{j^3\omega^3 L_s L_p C_r}{R_{eq}} + j^2\omega^2 L_s C_r + \frac{j^2\omega^2 R L_p C_r}{R_{eq}} + \frac{j^2\omega^2 L_p C_r}{Rj\omega C_r + \frac{j^3\omega^2 C_r X L_p}{R_{eq}} + j^2 X\omega C_r}} \quad (17)$$

where $C_r = 2C_c$.

The final step involves substituting the following normalising factors $L_p = AL_s$, $L_s C_r = 1/{\omega_0}^2$, $L_s/R_{eq} = Q/\omega_0$ and $f_n = \omega/\omega_0$ to obtain:

$$M_{g(clmp)} = \frac{{f_n}^2 A}{{f_n}^2 A + {f_n}^2 - B + k_r + j({f_n}^3 AQ - f_n AQB + k_i)} \quad (18)$$

where $k_r = \omega C_r(f_n AQR + X)$ and $k_i = \omega C_r(-R + f_n AQX)$, are terms accounting for the change in the effective impedance of the C_c caused by the diode-clamp when it is active. In the absence of diode-clamp ing (i.e. normal operation), $R = 0$ where $X = -1/(2\omega C_c)$, $k_r = -1$ and $k_i = -f_n AQ$, and (18) then simplifies to (6).

3 Operation characteristics

From (18), a plot of the first stage converter voltage gain under various overloading conditions is shown in Fig. 5 (a). The results show that during normal loading conditions the gain is unaffected. As the loading condition increases beyond the maximum, gains around the LIP begin to reduce as a function of the overloading condition. The normalised gain versus the normalised load resistance is shown in Fig. 5 (b), where it is seen that as the loading condition increases (i.e. lower load resistance), the gradient approaches unity.

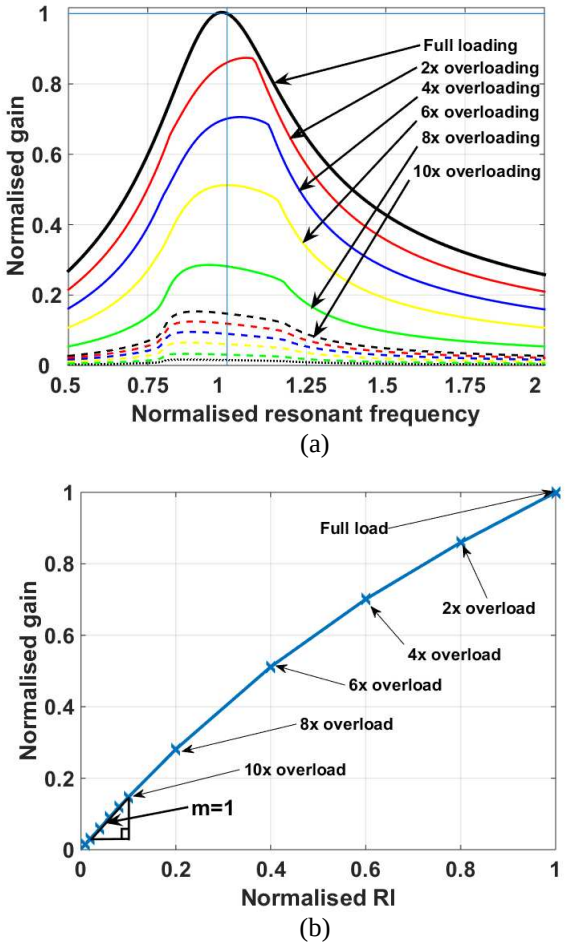

Fig. 5: Voltage gain characteristic of the first stage.

This is indicative of the converter characteristics changing from a constant voltage source into a constant current source under heavy overloading conditions, allowing both desired

charging modes to be realised. With ideal lossless components, no voltage and current regulation is required for the two stages when operating at the load independent point.

The V-I characteristic of the first stage under various loading and overloading conditions is shown in Fig. 6, and indicates the difference in voltage in the two operating modes. To compensate for this, the second stage converter includes a switching mechanism to reduce the voltage gain in the CV mode to that in CC mode.

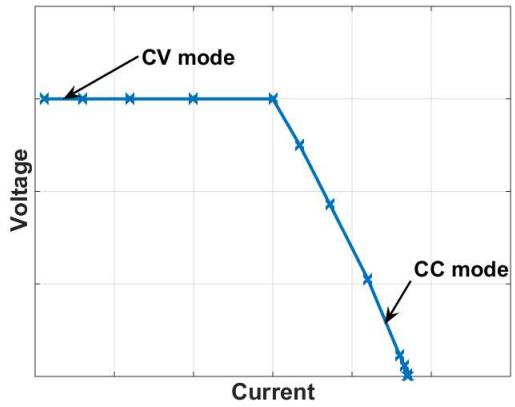

Fig. 6: V-I characteristic of the proposed converter.

This is better illustrated in Fig. 7. The gain is initially unity at the LIP. After a step increases in the transforer turns ratio, the gain is reduced inversely proportional to n. Using (3), the second stage gain under various switching frequency and loading condition can be found, thereby allowing both line and load regulation to be performed.

Due to the change in the equivalent load condition and transformer parameters as the turns ratio is changed, an additional resonant tank capacitor is included to keep the resonant frequency constant.

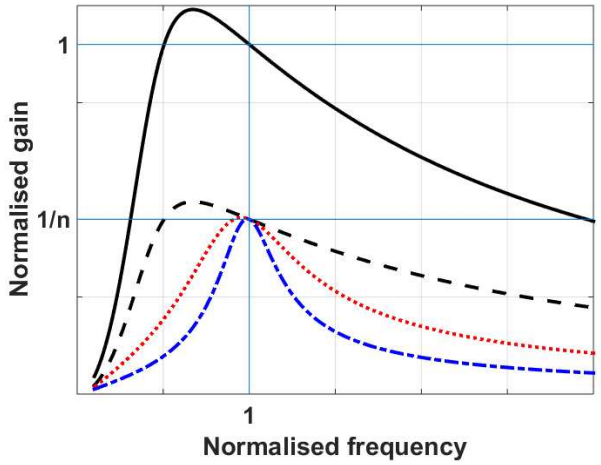

Fig. 7: Gain characteristic of the second stage.

4 Design example

A battery charger requiring a power rating of 2.5 W (1.4V, 1.8A), with an input voltage of 30V, is designed. Using (1) and with the resonant frequency of 100 kHz and turns ratio of (primary:secondary) 2:1, the resulting resonant tank components for the first stage are: L_{p1} = 119 μH, L_{s1} = 24 μH, C_{c1} = 5.4 nF. The second stage is also operating at the same switching frequency and its tank components are, by design, L_{p2} = 8.0 μH, L_{s2} = 1.6 μH, C_{c2} = 804 nF. Operating characteristics are plotted in Fig. 8 (a) and (b), showing that the converter can function both in constant current and constant voltage modes.

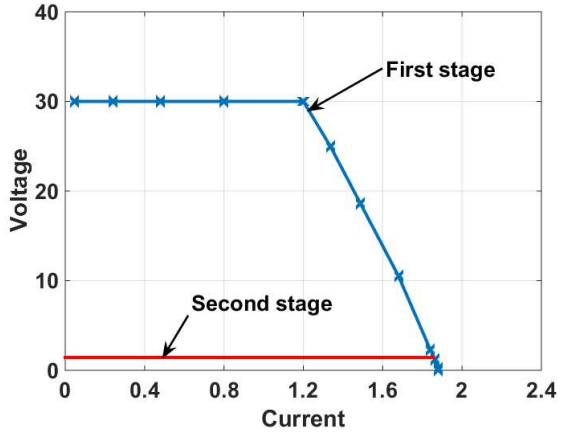

(a)

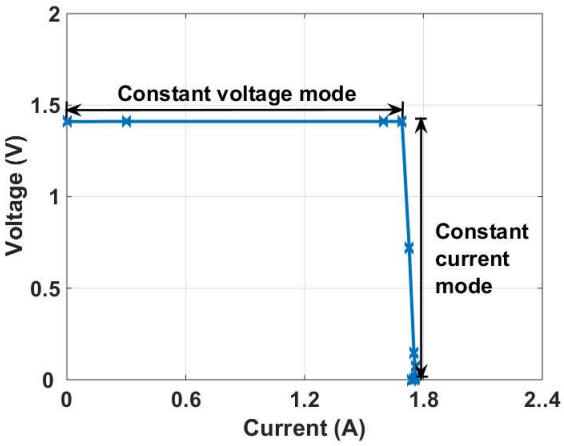

(b)

Fig.8: V-I characteristic of the proposed converter. (a) two stages independent (b) two stages combined

The two stages of the commissioned prototype converter are shown in Fig. 9 (a) and (b) respectively.

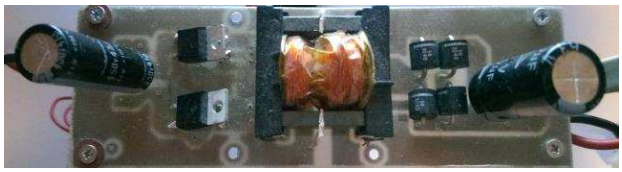

(a)

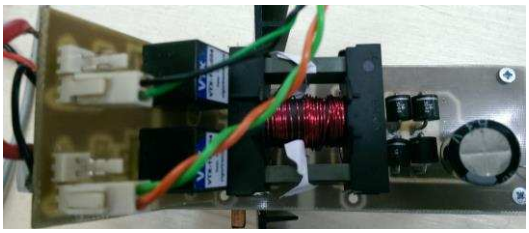

(b)

Fig. 9: Pictures of the prototype converter. (a) first stage (b) second stage

Four AA batteries with the rated capacity of 1.3 AH each are charge with the proposed converter, with the charging waveforms over the first 10 minutes shown in Fig. 10. The results show the expected behaviour of a battery being charged.

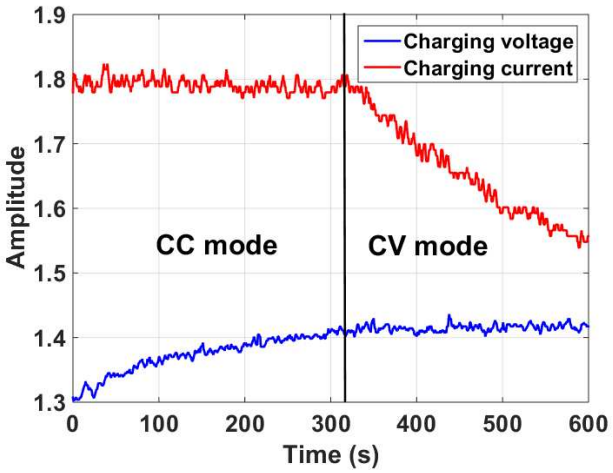

Fig. 10: Experimental result of the proposed battery charger.

5 Conclusion

This paper demonstrates a capacitor-diode-clamp LLC resonant converter which facilitates both constant voltage and constant current modes of operation typically required for battery charging. A second stage is incorporated to obtain the gain required for constant current mode operation. A design example is given. The included experimental result of the battery charging demonstrates the robustness of proposed converter and its current limiting characteristic. The benefit of this proposed charger is that it cannot go above the maximum charging current after the design stage. No current protection is required.

References

[1] M. Yilmaz, P.T. Krein. "Review of Battery Charger Topologies, Charging Power Levels, and Infrastructure for Plug-in Electric and Hybrid Vehicles", IEEE Trans. Power Electron., **Vol.28**, PP. 2151-2169, (2013),

[2] R.L. Steigerwald. "A Comparison of Half-bridge Resonant Converter Topologies", IEEE Trans. Power Electron., **Vol. 2**, pp. 174-182, (1988).

[3] C.W. Tsang, M.P. Foster, D.A. Stone, D.T. "Analysis and Design of LLC Resonant Converters with Capacitor-Diode Clamp Current Limiting", IEEE Trans. Power Electronics., **Vol.30**, PP. 1345-1355, (2015),

[4] B. Yang, F.C. Lee, M. Concannon. "Over current protection methods for LLC Resonant Converter", IEEE Conf. APEC 2003, PP. 605-609, (2003).

[5] K. Colak, E. Asa, D. Czarkowski. "Dual Closed Loop Control of LLC Resonant Converter for EV Battery Charger" IEEE conf. ICRERA 2013, PP. 811-815, (2013).

[6] J. Deng, S. Li, S. Hu, C.C. Mi, R. Ma. "Design Methodology of LLC Resonant Converters for Electric Vehicle Battery Chargers", IEEE Trans. Vehicular Tech., **Vol.63**, PP. 1581-1592, (2014).

[7]http://batteryuniversity.com/learn/article/charging_the_lead_acid_battery